Optimization of reliable cyclic cable layouts in offshore wind farms

Arne Klein and Dag Haugland

Department of Informatics, University of Bergen, Bergen, Norway

ABSTRACT

A novel approach for optimizing reliable cable layouts in offshore wind farms is presented. While optimization models traditionally are designed to suggest acyclic cable routes, those developed in this work recognize that cyclic layouts reduce the consequences of cable failures. The models under study take into account that cables cannot cross each other, which, particularly in instances with restrictive cable capacity, can make it attractive to let cables follow a joint trajectory, and visit turbines without connecting to them. A two-layered optimization process is developed. The outer layer is associated with an integer programming problem, which is subject to simultaneous generation of rows and columns representing cable paths. In the inner layer, a problem identifying feasible low cost paths is solved, guided by optimal dual variable values in the continuous relaxation of the former problem. Results from experimental applications to existing wind farms show good promise of the method.

1. Introduction

Wind energy has been the most steadily growing energy sector in the European Union in the last 15 years. In 2015 and 2016, it overtook hydro and coal power generation capacity in the EU, and is now the second largest energy sector after natural gas. Offshore wind energy made up about 10% of the installed wind capacity in 2017, with a growing market share (WindEurope 2017).

As of 2017, the first bid for large-scale subsidy-free offshore wind farms was made by Ørsted, committing to build two 240 MW projects, which are planned to be in operation by 2024 (Dong Energy 2017). Later, Vattenfall was also awarded contracts to develop subsidy-free offshore wind farms (CleanTechnica 2019): Hollandse Kust Zuid 1&2 offshore wind farms, with a total capacity of up to 750 MW, are planned to become operative in 2022. According to this plan, they will be the first subsidy-free offshore wind farms to go into operation. In 2019, Vattenfall won the contract also to develop Hollandse Kust Zuid 3&4 (up to 760 MW) without subsidies. Even though projects without subsidies are emerging, and the levelized cost of energy (LCOE) of offshore wind energy has been drastically reduced over the last decade, the challenge of reducing costs remains.

By optimizing the layout of offshore wind farms, the LCOE can be cut. This is accomplished either in terms of reductions in the investment, operational or maintenance costs, or by increasing the energy yield. In wind farms characterized by homogeneous soil conditions, optimal turbine placement has little effect on the construction costs, and will mainly be targeted at increased power production (Larsen *et al.* 2011). In contrast to that, the purpose of optimizing the routes of intra-array power cables, which connect the turbines to power substations, is to cut the construction costs. Fagerfjäll (2010) and Pillai *et al.* (2015, 2017) study how cable routes and turbine positions can be optimized concurrently. This requires a complex cost model, setting construction costs into context

---

with power production, and possibly including fatigue calculations, operations and maintenance, and more (Larsen *et al.* 2011).

A cyclic cable layout, also referred to as a closed-loop structure (Fischetti and Pisinger 2018b), entails higher construction costs of the wind farm, but can compensate financially in terms of improved reliability. In the case of a cable failure, the repair process may be time consuming because specialized vessels and crew have to be available and the maintenance operations require favourable weather conditions. The advantage of a *reliable cyclic cable layout* is that the wind turbines can continue to operate by using the alternative path for power transport. The economic advantage of being able to produce power in the case of failure can outweigh the additional construction costs of reliable cabling. Cyclic cable routes also have a technological advantage. Many electronic power components require grid synchronicity, and the loss of grid connection can therefore damage these components. Either a cyclic (reliable) or an acyclic and possibly ramified (branching) cable layout must be used. Which of these to choose has to be determined in the planning phase of an offshore wind farm, taking into account, amongst other things, expected failure rates, repair times and loss of production.

The goal of the present work is to compute intra-array cable layouts in offshore wind farms such that the costs are minimized. The focus is on instances where reliable cable layouts are required, and to be accomplished by means of *cyclic cable paths*. Not only do the turbines have to be connected to a substation by a cable, they also have to remain connected in the case of a cable breakdown occurring. In the presumably unlikely event of multiple failures on the same cable, it is however not guaranteed that every turbine remains connected. The approach taken is thus that the *redundancy level* of the cable layout is fixed. Trade-off between shortfall in production revenues and costs in enhanced reliability is consequently disregarded.

Operation and maintenance constitute a major part of the lifetime costs of offshore wind-farm projects. Such cost components are also strongly correlated with the cable laying costs, which in their turn depend heavily on the cable length and type. Omission of costs incurred in the operational phase is therefore not likely to introduce a strong bias in the comparison of two alternative cable layouts, given that they have identical redundancy levels. For the purpose of simplicity and model tractability, the study is consequently confined to costs incurred in the construction phase, while implications that the choice of routes might have on operation, maintenance and fatigue are neglected.

1.1. Literature review

Since the frequently cited work by Mosetti, Poloni, and Diviacco (1994), a large number of research articles on optimization of *turbine locations* have emerged. Approaches that have been applied include various metaheuristic methods, such as genetic algorithms (Grady, Hussaini, and Abdullah 2005; Emami and Noghreh 2010; Chen *et al.* 2013; Pillai *et al.* 2016, 2017), particle swarm optimization (Chowdhury *et al.* 2013; Pillai *et al.* 2018), simulation of viral life (Ituarte-Villarreal and Espiritu 2011) and evolutionary algorithms (González *et al.* 2010; Rodrigues, Bauer, and Bosman 2016). Optimized turbine location has also been approached by pattern search (Du Pont and Cagan 2012), simulation (Marmidis, Lazarou, and Pyrgioti 2008), and mathematical programming techniques, such as linear (Fagerfjäll 2010) and quadratic (Quan and Kim 2019) integer programming, and constraint programming (Zhang *et al.* 2014). For an overview of research on optimized turbine location in onshore and offshore wind farms, published before 2014, the reader is referred to the survey by Herbert-Acero *et al.* (2014).

Research on the optimization of *cable layouts* in offshore wind farms has proved that mixed integer linear programming (MILP) models are powerful tools. Works in this vein include models based on minimum Steiner tree (Fagerfjäll 2010) and capacitated spanning tree (Lindahl *et al.* 2013; Svendsen 2013) problems, as well as the capacitated clustering model developed by Pillai *et al.* (2015). The model presented by Lindahl *et al.* (2013) is the basis for Ørsted's cabling methodology. Metaheuristic methods, especially genetic algorithms (Lingling, Yang, and Xiaoming 2009; Gonzalez-Longatt *et*

al. 2012; Pillai *et al.* 2016; Shin and Kim 2017), and, more recently, particle swarm methods (Pillai *et al.* 2018) have also been applied for optimizing turbine locations and cable routes connecting the turbines.

According to Pillai *et al.* (2015) and Fischetti and Pisinger (2018a, 2018b, 2018c, 2019), a number of limitations apply to possible cable lines. Each cable can only transport a certain amount of power, which imposes an upper bound on the number of turbines connected to it. The maximum number of turbines per cable is decided upfront, taking into account the power losses caused by this choice. In addition, cable crossings are disallowed due to technical limitations: the mooring process of the cables would become significantly more complex with cable crossings, and maintenance and repairs would become more difficult and expensive. Cable cost can be reduced by minimizing the total cable length in the wind park.

Recent scientific publications (Lindahl *et al.* 2013; Bauer and Lysgaard 2015; Klein *et al.* 2015; Pillai *et al.* 2015, 2016, 2018; Cerveira, Baptista, and Pires 2016; Cerveira *et al.* 2016; Wędzik, Siewierski, and Szypowski 2016; Hertz *et al.* 2017; Fischetti and Pisinger 2018a, 2018b, 2018c, 2019; Klein and Haugland 2019) assume that all turbines are connected to substations in a tree with the substation as the root node. From each turbine therefore, there exists a unique cable path to the substation. Bauer and Lysgaard (2015) introduce an integer programming (IP) model with hop-indexed variables, resembling a planar open vehicle routing problem. However, their formulation does not allow for branching at the turbine nodes. The resulting layouts are trees without branches, which is a directed star, with the substation as the root.

MILP models supporting ramified cable routes, where branching at turbine nodes is allowed, are introduced by Pillai *et al.* (2015), Klein *et al.* (2015), Wędzik, Siewierski, and Szypowski (2016) and Fischetti and Pisinger (2018a, 2018b). Pillai *et al.* (2015) also suggest a way to handle obstacles, by calculating the shortest path between pairs of turbines, taking into account obstacles, in a pre-processing step. This technique is useful for handling realistic instances with realistic costs. It does, however, not change the optimization model.

To avoid cable routes intersecting forbidden areas on the seabed, including physical obstacles, Fischetti and Pisinger (2018b) introduce optional connection points at the boundary of such areas. By means of the additional points, referred to as *Steiner* points, the best obstacle-avoiding cable routes can be assessed. Fischetti and Pisinger (2018c) further extend the MILP model by incorporating future reduced revenues due to power losses. Independently of the above work, the idea of Steiner points is also applied by Klein and Haugland (2019). They present a model where segments of different cables are allowed to share a joint trajectory, and cables can be laid in the close vicinity of turbines they do not connect. The latter is achieved by introducing Steiner points on arbitrarily small circles centred on the turbine locations to which the cables are allowed to connect. A similar method is applied to allow for (multiple) cables laid around obstacles.

The reliability of cable layouts is an important feature that does not appear to have been studied extensively in the optimization literature. As pointed out by Wei *et al.* (2017), cyclic layouts have been used in several cases, for example in the London Array and Robin Rigg offshore wind farms (The Kingfisher Information Service—Offshore Renewable & Cable Awareness Project (KIS-ORCA) 2016a, 2016b). Quinonez-Varela *et al.* (2007) compare different types of offshore wind-farm layout, including reliable and ramified layouts, and highlight the advantages of reliable ring-layouts with a structure as introduced in Section 1. While targeting the needs for a particular company, Fischetti and Pisinger (2018b) propose an optimization model supporting cyclic cables. Their implicit assumption is that the wind farms have a single substation, in contrast to, for example, the London Array instance. Gong, Kuenzel, and Pal (2018) develop particle swarm methods adapted to instances demanding a possibly higher redundancy level than is offered by purely cyclic cables. Compared with the ring layout, the multi-loop layouts studied by Gong, Kuenzel, and Pal (2018) have additional cable connections, increasing the reliability further. More failures are tolerated before turbines are disconnected, but such structures also increase the cable costs significantly.

1.2. Contributions

A review of the literature on the optimization of cyclic cable layouts for offshore wind farms reveals the following gaps.

(1) Following Fischetti and Pisinger (2018b), it is straightforward to extend hop-indexed formulations (Bauer and Lysgaard 2015; Klein and Haugland 2019) such that they account for reliable cyclic cable layouts. In instances where multiple substations are allowed, however, the extension implies a duplication of the binary variables over the set of substations. This is likely to render the model size intractable for general-purpose solvers, and calls for tailored solution strategies.

(2) Because of the non-crossing constraints, the route of one cable represents an obstacle to other cables. The optimization model must respect such *endogenous obstacles*, in addition to any exogenous ones. As a result, whenever costs can thus be cut, two cable trajectories should partly coincide. Figure 1 depicts one such instance, where the solution with partly joint trajectories (right) incurs a lower cost than the one without (middle). Joint trajectories complicate the modelling of the non-crossing requirements (see Section 2), and the scientific literature seems to offer no study of cyclic cable layouts where this feature is incorporated.

In this work, contributions to the literature on cable layout optimization in offshore wind energy are made by closing the above gaps. First, a model supporting reliable cable layouts is formulated. That is, all turbines are connected to the substation by cyclic cables, the routes of which are allowed to coincide. Second, a novel path-based model and an associated solution procedure are developed, along with numerical experiments examining the computational performance of the procedure.

Reflecting the possibility of joint cable trajectories, it is necessary to distinguish between *connecting* and *non-connecting* cables *visiting* a turbine. In any feasible cable layout, each turbine is visited by exactly one connecting cable, and any number (zero or more) of non-connecting ones. In the solution in Figure 1 (right), the turbines closest to the substation are visited by both of the cables, but connected only by the short cable (solid line). The turbines located remotely from the substation are visited only by the long cable (dashed line), which also connects them. Between the substation and the closest turbines, the two cables follow a joint trajectory.

In what follows, two cables are said to be *parallel* if they partly share a joint trajectory. Practical implementations of parallel cables require a physical separation between them, such that their trajectories will not be exactly identical. Small practical adjustments of the optimized cable layout may also be necessary to account for other technical details, such as bend radii and cable turns. It is assumed throughout the current text that such adjustments are too modest to have a significant impact on the best choice of cable layout, and will consequently not be considered further. Owing to the needs for isolation and cable repair for example, cables must be laid at some minimum distance from the turbines that they do not connect. Therefore, the presence of non-connecting cables visiting a turbine might induce practical adjustments of the cable routes, which also are assumed to be negligible. Near
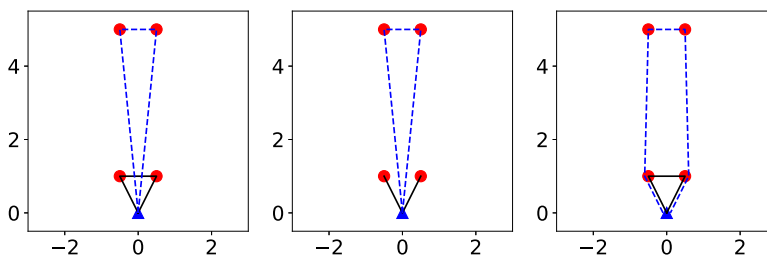
Figure 1. Example of a case where parallel cables give a better solution. Left: disallowed due to cable crossings. Middle: feasible solution without cable crossings. Right: improved solution with parallel cables.

the substations, it might be necessary to modify the cable trajectories in such a way that their angular separation is sufficient. This also falls into the category of adjustments that are assumed to be made after optimization of the cable layout, and is consequently not incorporated in the analysis to follow. It is further assumed that none of the adjustments incur extra costs.

The article is organized as follows. In Section 2, the problem is defined in precise mathematical terms. The master problem and the subproblem, as well as the iterative algorithm exploiting the solutions to both problems, are explained in detail in Section 3. In Section 4, the experiments that have been conducted are described, and experimental results are presented.

2. Problem definition

Before describing in detail the problem to be solved, this section introduces the notation which is used throughout the article. It is assumed that a set T of turbine nodes and a set D of substation nodes are given. The node set is denoted $N = D \cup T$. Together with the set $A \subseteq N \times N$ of arcs, representing the possible cable connections between the nodes, the node set defines a directed graph $G = (N, A)$. The set of end nodes of arcs leaving node $i \in N$ is denoted $N_i^+ = \{j \in N : (i, j) \in A\}$, and the set of start nodes of arcs entering i is denoted $N_i^- = \{j \in N : (j, i) \in A\}$. Let C_T denote the maximum number of turbines a single cable line can connect. For simplicity, it is assumed that all cables have the same cross-section, and thereby that the bound C_T applies to all cable lines. As explained in Section 1.2, any given cable subdivides the set of turbines it visits into two subsets, such that the first contains all turbines that the cable connects, and the second contains the turbines connected by some other visiting cable. Let $C_N \in [C_T, |T|]$ denote an upper bound on the total number of turbines a cable can visit.

In this text, a *path* p in G is understood to be a pair $(N(p), T(p))$ consisting of

- a sequence of nodes on the form $N(p) = (d_p, t_p^1, \ldots, t_p^m, d_p)$, where $d_p \in D$, $t_p^1, \ldots, t_p^m \in T$ and $m \geq 1$ is the number of turbine nodes that the path p visits, and
- a non-empty subset $T(p) \subseteq \{t_p^1, \ldots, t_p^m\}$.

In this definition, p represents a cable line, $N(p)$ represents the substation and the turbines visited by the cable, the set $T(p)$ represents the turbines that the cable connects, and $N(p) \setminus T(p) \setminus D$ represents the visited turbines connected by other cables. The arc set of path p is denoted $A(p) = \{(d_p, t_p^1), \ldots, (t_p^m, d_p)\}$, and $G(p)$ denotes the corresponding directed subgraph. Let P be the set of paths p in G satisfying $|T(p)| \leq C_T$ and $|T \cap N(p)| \leq C_N$.

The injective function $L : N \mapsto \mathbb{R}^2$ defines the embedding of the nodes in the plane. Correspondingly, the embedding of an arc $(i, j) \in A$ is the closed line segment from $L(i)$ to $L(j)$, written as $L[i, j] = \{L(i) + \lambda(L(j) - L(i)) : \lambda \in [0, 1]\}$. The corresponding open line segment is denoted $L(i, j) = \{L(i) + \lambda(L(j) - L(i)) : \lambda \in (0, 1)\}$. The embedding of a path $p \in P$ is the concatenation of the embedding of its arcs $A(p)$, and thus defined as $L(p) = \bigcup_{(i,j) \in A(p)} L[i, j]$. Further, the interior of the polygon bounded by $L(p)$ is denoted $I(p)$. A list of symbols introduced is given in Table 1.

The installation cost of the intra-array grid is composed of a number of different types of expense. However, many of those will be constant irrespective of the chosen cable layout, and thus do not need to be considered when optimizing intra-array cable layouts. For cyclic cable layouts, the number of turbine–cable connections is constant, as each turbine has exactly two cable connections. The focus of the current work is thus the variable costs, which are mainly incurred by the cables themselves and the trenching process. It is therefore reasonable to assume the costs to be approximately proportional to the cable length. The optimization problem is to find a cable layout, *i.e.* a set of cyclic cable paths fulfilling all requirements detailed below, which has a minimal total cable length.

Several requirements are imposed in the reliable intra-array cabling problem: to ensure delivery of the generated electricity, each turbine $t \in T$ must be connected to a substation $d \in D$ by a cable $p \in P$. Reliability of the cable paths implies that there must be two distinct paths for the electricity

Table 1. Nomenclature.

| Symbol	Explanation
T	Set of turbine nodes
D	Set of substation nodes
N	Set of nodes ($N = T \cup D$)
A	Set of arcs representing possible cable segments
G	Digraph representing possible cable layouts ($G = (N, A)$)
P	Set of feasible paths in G
N_i^+	Out-neighbours of node i in G
N_i^-	In-neighbours of node i in G
C_T	Cable capacity, *i.e.* an upper bound on the number of turbines to which a cable can connect
C_N	An upper bound on the number of turbines a cable path can visit
$N(p)$	The cyclic sequence of nodes visited by cable path p
$T(p)$	The set of turbines connected by cable path p
$A(p)$	The set of arcs in path p
$G(p)$	The graph with node set $N(p)$ and arc set $A(p)$ corresponding to path p
$L(i)$	The plane embedding (coordinates) of node i
$L(i,j)$	The plane embedding (open interval) of arc (i,j)
$L[i,j]$	The plane embedding (closed interval) of arc (i,j)
$L(p)$	The plane embedding of path p
$I(p)$	The interior of the polygon bounded by $L(p)$
χ_p	The set of paths crossing path p
Γ	The set of crossing arc pairs
c_{ij}	The length of a linear cable segment $L[i,j]$
c_p	The length of the cable corresponding to path p

transported from each turbine. Cyclic cables enable continued use of all turbines without restrictions in the case of a single cable failure. For simplicity, the cyclic routes are assumed to be fully rated, such that, in the event of a single cable failure, full power can still be exported. Also in the case of a turbine failure, which cuts power transport in the turbine, all other turbines can continue to operate. In graph theory terms, each subgraph $G(p)$ must be a cycle intersecting D.

The following three categories of disallowed cable crossing are considered.

(1) Arc crossing: for some arcs $(i,j) \neq (i',j')$, $L(i,j)$ and $L(i',j')$ intersect. That is, $L(i,j) \cap L(i',j') \neq \emptyset$.
(2) Node crossing: for paths p and p', where p contains arcs (i,t) and (t,j), and p' contains arcs (i',t) and (t,j'), conditions $L(j') \in I(p)$ and $L(i') \notin I(p) \cup L(p)$ hold.
(3) Path crossing: for paths p and p', where, for an integer $k \geq 1$ denoting the number of turbines visited jointly by p and p', p contains arcs $(i,t_1),(t_1,t_2),\ldots,(t_{k-1},t_k),(t_k,j)$, and p' contains arcs $(i',t_1),(t_1,t_2),\ldots,(t_{k-1},t_k),(t_k,j')$, conditions $L(j') \in I(p)$ and $L(i') \notin I(p) \cup L(p)$ hold.

Node crossing is a special case of path crossing ($k = 1$). The categories are illustrated in Figure 2.

Arc crossing is avoided by constraints defining two arcs to be mutually exclusive. In optimization models that are formulated in terms of binary variables defined over the arc set, crossing of two given
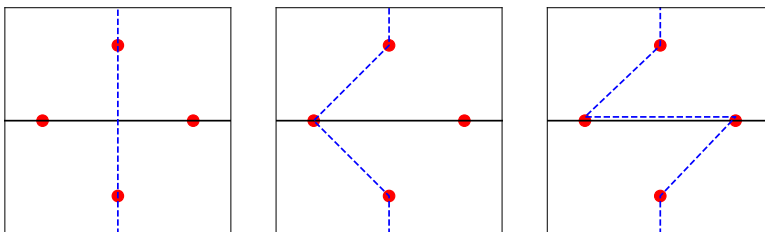
Figure 2. Illustration of different types of cable crossing. Left: arc crossing. Middle: node crossing. Right: path crossing.

arcs is avoided by restricting the sum of the corresponding variables to be no more than one. This applies not only to models consisting uniquely of binary variables (Bauer and Lysgaard 2015; Klein and Haugland 2019), but also to models containing continuous power flow variables (Pillai *et al.* 2015; Fischetti and Pisinger 2018a, 2018b, 2018c, 2019). To disallow node crossings, constraints excluding at least one out of four arcs are required. Further intractability occurs when considering path crossing, the avoidance of which requires constraints involving an arbitrary number of variables.

Constraints corresponding to all cable crossing categories are formulated straightforwardly in terms of path variables. To that end, the following formal definition of mutually exclusive paths is useful.

Summarizing the crossing categories (1)–(3) above, two paths $p, p' \in P$ are said to be crossing if and only if $G(p) \neq G(p')$ and both of the following conditions are fulfilled.

- The interior of the bounded regions enclosed by the paths overlap, *i.e.* $I(p) \cap I(p') \neq \emptyset$.
- None of the paths are embedded entirely within the bounded region enclosed by the other path. That is, $L(p) \setminus L(p') \setminus I(p') \neq \emptyset \neq L(p') \setminus L(p) \setminus I(p)$.

Define $\chi_{p'} = \{p \in P : p \text{ crosses } p'\} \subset P$ as the set of paths crossing path $p' \in P$, and Γ as the set of arc pairs $(i_1, j_1), (i_2, j_2)$ satisfying the definition of an arc crossing.

For arc $(i, j) \in A$, define the length (also referred to as the cost) $c_{ij} = \|L(j) - L(i)\|_2$ as the Euclidean distance between its end nodes. It is assumed that the cable cost is proportional to the cable length, and that the length $c_p = \sum_{(i,j) \in A(p)} c_{ij}$ of the path embedding $L(p)$ represents the cost of path $p \in P$.

The problem under study can now be formulated as follows: find a set of paths $P^* \subseteq P$ such that

- $\{T(p) : p \in P^*\}$ is a partition of T, *i.e.* for all $t \in T$, there is a unique $p \in P^*$ such that $t \in T(p)$,
- if $p, p' \in P^*$, then $p \notin \chi_{p'}$ and $p' \notin \chi_p$, and
- $\sum_{p \in P^*} c_p$ is minimized.

3. Solution method

As indicated in Section 2, the non-crossing constraints are easy to formulate in terms of binary variables defined over the path set P. However, the number $|P|$ of such path variables is exponential in the number $|T|$ of turbines. In the worst case, the number of conflicts between crossing paths in P also grows exponentially with $|T|$. A model formulation including all variables and all non-crossing constraints is thus intractable to MILP-solvers.

3.1. Overview of the solution approach

Exponential growth in variables and constraints calls for a solution method that inherits from both *column generation* and *row generation*. However, traditional column-generation methods do not apply. This is because the generation of a new path (column) requires also that a set of new constraints be added, namely the non-crossing constraints involving the newly generated path. Analogously, constraint generation techniques fall short because they fail to identify new paths to be added. Examples include the iterative procedures for generating crossing constraints studied by, for example, Pillai *et al.* (2015), Lindahl *et al.* (2013) and Bauer and Lysgaard (2015). Whereas these procedures generate only rows, an algorithm that generates rows and columns simultaneously is developed in the current work.

The solution procedure developed below consists of two layers, each of which identifies an optimization problem. By solving the *subproblem*, cable paths in P are identified. Paths thus encountered are represented by a corresponding variable (column) in the *master problem*. They also induce

master problem constraints excluding pairs of crossing paths. A solution to the master problem then represents an optimal subset of generated paths.

The solution algorithm repeatedly solves instances of the two problems. Each instance of the master problem is identified by a subset $\bar{P} \subseteq P$ of paths in G. In the hypothetical case where $\bar{P} = P$, the optimal solution to the master problem is also the solution to the problem defined in Section 2. Otherwise, only a feasible solution is guaranteed. By gradual extensions of $\bar{P}$, the optimal cost in the master problem instance decreases. It does, however, not necessarily run until $\bar{P}$ contains an optimal solution P^*, and hence it does not guarantee that the original problem is solved to optimality.

3.2. Master problem

For each path $p \in \bar{P}$, define the decision variable v_p such that $v_p = 1$ if path p is used, and $v_p = 0$ otherwise. Let $\bar{\chi}_p = \chi_p \cap \bar{P}$ denote the set of paths in $\bar{P}$ that cross path $p \in \bar{P}$. An optimal subset of cable paths in $\bar{P}$ is found by solving the following integer program:

$$\min \quad \sum_{p \in \bar{P}} c_p v_p \tag{1}$$

$$\text{s.t.} \quad \sum_{p : t \in T(p)} v_p = 1 \quad \forall\, t \in T, \tag{2}$$

$$v_p + \frac{1}{|\bar{\chi}_p|} \sum_{p' \in \bar{\chi}_p} v_{p'} \leq 1 \quad \forall\, p \in \bar{P}, \tag{3}$$

$$v_p \in \{0, 1\} \quad \forall\, p \in \bar{P}. \tag{4}$$

Constraint (2) assures that every turbine is connected by exactly one path, while constraint (3) guarantees that no two crossing paths are part of the solution. A stronger version of this constraint is the formulation $v_p + v_{p'} \leq 1$ for all pairs (p, p') of crossing paths. Formulation (3) has, however, the following advantages: first, the number of constraints is linear in the number of paths, and only one new constraint needs to be generated when $\bar{P}$ is extended by one new path; second, and as explained below, the formulation enables the extraction of information about the value of avoiding crossings with any given path in $\bar{P}$.

3.2.1. The continuous relaxation and its dual

Consider the continuous relaxation of problem (1)–(4), and denote by μ_t, $t \in T$, the dual variable corresponding to (2). Large positive values of μ_t indicate that it is expensive to connect turbine t by one of the paths currently in $\bar{P}$, and suggest that $\bar{P}$ be extended by some $q \in P \setminus \bar{P}$, where $t \in T(q)$. The dual variable corresponding to (3) is denoted by η_p, $p \in \bar{P}$. It is interpreted as the negative of the marginal cost of having to avoid all paths in $\bar{\chi}_p$. Thus, large values of $-\eta_p$ discourage extensions of $\bar{P}$ by crossing paths $q \in \chi_p \setminus \bar{P}$.

Besides the non-positivity of η_p ($p \in \bar{P}$), the dual constraints of the continuous relaxation of the master problem read

$$\sum_{t \in T(p')} \mu_t + \eta_{p'} + \sum_{p \in \bar{\chi}_{p'}} \frac{1}{|\bar{\chi}_p|} \eta_p \leq c_{p'} \quad \forall\, p' \in \bar{P}. \tag{5}$$

3.3. Subproblem

The master problem in Section 3.2 relies on a mechanism for generating new and unexplored paths, by which the path set $\bar{P}$ is to be extended. Identifying the best new path is referred to as the *subproblem*.

3.3.1. Path formulation of the subproblem

Consider an arbitrary path $q \in P \setminus \bar{P}$ and an optimal dual solution (μ, η) to the continuous relaxation of (1)–(4). Because $q \notin \bar{P}$, (3) does not apply to (is not binding for) path q, and $\eta_q = 0$ can be assumed. Following the idea of column-generation algorithms, q can be priced into $\bar{P}$ if the dual constraint corresponding to q is violated, *i.e.* if

$$c_q - \sum_{p \in \bar{\chi}_q} \frac{1}{|\bar{\chi}_p|} \eta_p - \sum_{t \in T(q)} \mu_t < 0.$$

Identifying such a path, or concluding that none exists, is accomplished by solution of the subproblem

$$z(\bar{P}) = \min \left\{ c_q - \sum_{p \in \bar{\chi}_q} \frac{1}{|\bar{\chi}_p|} \eta_p - \sum_{t \in T(q)} \mu_t : q \in P \setminus \bar{P} \right\}. \tag{6}$$

If $z(\bar{P}) < 0$, $\bar{P}$ is extended by a path q for which the minimum is attained. Otherwise, the optimal objective function value of the relaxed master problem cannot be reduced by further extensions of $\bar{P}$, and the column-generation process is concluded.

3.3.2. Node rewards and modified arc costs

Problem (6) is recognized as a constrained shortest-path problem, which acknowledges the reward μ_t to paths q that connect turbine t. Costs are incurred according to the total arc costs $c_q = \sum_{(i,j) \in A(q)} c_{ij}$, and a penalty $-\eta_p/|\bar{\chi}_p|$ for each path $p \in \bar{\chi}_q$.

To formulate (6) as a binary program with variables associated with arcs, the penalty $-\eta_p/|\bar{\chi}_p|$ must be attributed to one of the arcs in q. In the case of an arc crossing between $(i_p, j_p) \in A(p)$ and some $(i_q, j_q) \in A(q)$, arc (i_q, j_q) is chosen. In the case of a node or path crossing between p and q, it is less straightforward to assess where to assign the penalty. Denote by ξ_p the set of arcs to which the penalty $-\eta_p/|\bar{\chi}_p|$ is imputed. It follows that ξ_p contains all arcs crossing some arc in $A(p)$, but to reflect node and path crossings, it may also contain others, as detailed in the next section.

The set of paths included in $\bar{P}$ incurring a penalty on an arc $(i, j) \in A$ is reciprocally given as

$$\Xi_{ij} = \{p \in \bar{P} : (i, j) \in \xi_p\}.$$

3.3.3. Node and path crossings

To complete the assessment of ξ_p, it is shown in this section how all crossing categories between path p and some other path, q, can be represented in terms of arc crossings. By small perturbations of the path embeddings, the routes of p and q are transformed into slightly separated routes, even if the original embedding of p and q partly coincide. Further, by careful choice of the perturbing function, the separated routes intersect at one point if and only if $q \in \chi_p$ (the two cables cross according to the definition in Section 2). If an intersection is detected, the arc containing the intersection point is included in the set ξ_p. Otherwise, because of the absence of crossings between p and q, it is concluded that the two paths can be selected simultaneously.

Consider a function $\widetilde{L} : N \mapsto \mathbb{R}^2$, where $\widetilde{L}(i) = L(i)$ for all nodes $i \in D \cup (N \setminus N(p))$, and $\widetilde{L}(t) \approx L(t)$ for $t \in N(p) \setminus D$. That is, for all turbine nodes t visited by path p, $\widetilde{L}(t)$ is a slight perturbation of the original embedding $L(t)$ in the plane. At all other nodes, the new embedding coincides with the original. For the sake of simple notation, the dependency of $\widetilde{L}$ on p is suppresed. The idea behind $\widetilde{L}$ is that each node or path crossing p is to be transformed into an arc crossing. Define $\widetilde{L}(i, j)$, $\widetilde{L}[i, j]$ and $\widetilde{L}(p)$ $((i, j) \in A)$ analogously to $L(i, j)$, $L[i, j]$ and $L(p)$, respectively. If, for some $(i_p, j_p) \in A(p)$ and $(i, j) \in A$, $\widetilde{L}(i_p, j_p) \cap L(i, j) \neq \emptyset$, a crossing with p is attributed to arc (i, j), which accordingly is included in ξ_p.

For a precise definition of $\widetilde{L}$, consider a (small) real number $\epsilon > 0$. Consider also three consecutive nodes $i, t, j \in N(p)$ on path p, where t is a turbine node. Such nodes exist, even if p visits only one turbine, in which case $i = j \in D$. Define

$$\widetilde{L}(t) = L(t) \pm \frac{\epsilon}{\sqrt{2}} \left(\frac{L(i) - L(t)}{c_{ti}} + \frac{L(j) - L(t)}{c_{tj}} \right), \tag{7}$$

where the plus sign applies if $t \in T(p)$, and the minus sign applies if $t \in N(p) \setminus T(p)$. That is, $\widetilde{L}$ maps t to a point a distance ϵ from $L(t)$. If $t \in T(p)$, $\widetilde{L}(t)$ is located on the *internal bisector* of the angle between the vectors $L(i) - L(t)$ and $L(j) - L(t)$, whereas if $t \in T \setminus T(p)$, $\widetilde{L}(t)$ is located on the *external bisector* of the said angle. Consequently, if L embeds no three consecutive nodes of p on a joint straight line, and the polygon bounded by $L(p)$ is convex, then $\widetilde{L}(t) \in I(p)$ if and only if $t \in T(p)$. Hence, the transformation $\widetilde{L}$ maps t to some point in the interior $I(p)$ of the polygon bounded by $L(p)$ if p connects t, and maps the turbine to a point outside the polygon otherwise.

The perturbed embedding $\widetilde{L}$ is defined with respect to a given path p. Figure 3 illustrates $\widetilde{L}$ for two different choices of p. Consider the situation on the left, where only one path has been generated. Its perturbed embedding is shown by a solid line, which is seen (illustration in the middle) to fall inside the region bounded by the embedding of another path (dashed line). It is thus concluded that the two paths do not cross. On the right, the perturbed embedding with respect to the second path is also illustrated.

Consider a path q that makes a node or path crossing with p. The crossing implies that there exist nodes $i_q, j_q \in N(q)$ and $t \in T \cap T(p) \cap N(q)$ such that $(i_q, t), (t, j_q) \in A(q)$, and either $i_q \in I(p)$ or $j_q \in I(p)$. Assume $j_q \in I(p)$. For sufficiently small ϵ, $L(t, j_q)$ intersects $\widetilde{L}(p)$ at one of the two line segments incident to $\widetilde{L}(t)$, analogously to an arc crossing. In the case where $i_q \in I(p)$, an analogous argument shows that the embedding of arc (i_q, t) intersects the perturbed embedding of p at some point near $L(t)$.

Cases where paths p and q have turbine nodes in common, while $q \notin \chi_p$, are analysed next. Let $t_1, \ldots, t_k \in T \cap N(p) \cap N(q)$ be a sequence of $k \geq 1$ consecutive turbine nodes on both paths, and for $r = p, q$, let $i_r, j_r \in N(r)$ be adjacent nodes on path r satisfying $(i_r, t_1) \in A(r)$ and $(t_k, j_r) \in A(r)$, respectively. Assume $i_p \in I(q)$, which implies $j_p \in I(q)$, since $q \notin \chi_p$. Correspondingly, $i_q, j_q \notin I(p)$. If $t_1 \notin T(p)$, a better path than p is obtained by removing t_1. This would create no conflict with path q, since $L(i_p, t_2) \subset I(q)$. Therefore, $t_1, t_k \in T(p)$ can be assumed, yielding $\widetilde{L}[i_p, t_1], \widetilde{L}[t_k, j_p] \subset I(q)$, which means that neither $L[i_q, t_1]$ nor $L[t_k, j_q]$ intersects $\widetilde{L}(p)$. Thus, checking whether the embedding $L(i, j)$ of an arc (i, j) intersects the perturbed embedding $\widetilde{L}(p)$ of path p does not lead to false conclusions in instances where paths are laid partly in parallel.

Arc crossings are preserved by the perturbation $\widetilde{L}$ of the node embedding. If $L(i_p, j_p) \cap L(i, j) \neq \emptyset$ $((i_p, j_p) \in A(p), (i, j) \in A)$, then also $\widetilde{L}(i_p, j_p) \cap L(i, j) \neq \emptyset$ for sufficiently small ϵ. Likewise, $\widetilde{L}[i_p, j_p] \cap L[i, j] = \emptyset$ if $L[i_p, j_p] \cap L[i, j] = \emptyset$.
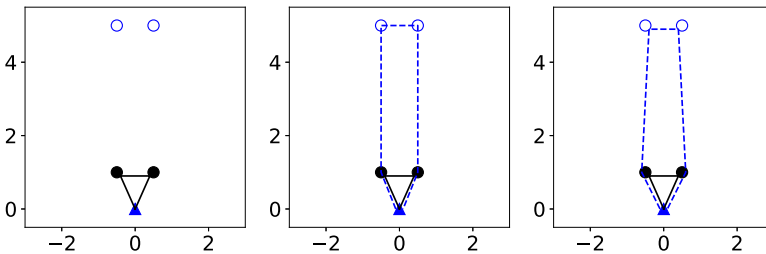
Figure 3. Illustration of the modified embedding $\widetilde{L}$ of two paths. The path drawn as a dashed line connects the two turbines at the top (unfilled circles). The path drawn as a solid line connects the two turbines in the middle (filled circles). The triangle represents the substation.

In conclusion, the set of arcs crossing p is defined as

$$\xi_p = \left\{ (i, j) \in A \setminus A(p) : \widetilde{L}(p) \cap L(i, j) \neq \emptyset \right\}.$$

3.3.4. Integer programming formulation of the subproblem

The subproblem (6) is formulated in terms of binary variables indexed by the arcs and the nodes in G, by means of which the path $q \in P \setminus \bar{P}$ to be found is represented. A set of the arc-indexed variables also have a hop index, resulting in a formulation that follows well-known principles of hop-indexed IP-models for acyclic, possibly ramified, cable layouts (Bauer and Lysgaard 2015; Klein *et al.* 2015; Klein and Haugland 2019). The hop-indexed variable x_{ij}^h ($h = 0, \ldots, C_N$, $(i, j) \in A$) equals one if (i, j) is the hth arc (counting starts at zero) on the path q from the substation in $N(q)$, and zero otherwise. The dependent variable y_{ij} equals one if $x_{ij}^h = 1$ for some $h = 0, \ldots, C_N$, and zero otherwise. Finally, z_t equals one if q connects turbine node t (if $t \in T(q)$), and zero otherwise.

As explained in Section 3.3.2, the objective function of the subproblem reflects not only the arc lengths, but also the optimal dual solution (μ, η) to the relaxation of the master problem. For the purpose of increased flexibility, define the real parameters k_μ and k_η representing the extent to which the dual solution is to be taken into account. Typical values of both parameters are in the interval $[0, 1]$. Variable z_t thus has objective function coefficient equal to $-k_\mu \mu_t$, while the coefficient of y_{ij} equals

$$\widetilde{c}_{ij} = c_{ij} - k_\eta \sum_{p \in \Xi_{ij}} \frac{1}{|\bar{\chi}_p|} \eta_p.$$

It is desirable to impose the generation of a path that connects a selected target turbine, which is denoted $\bar{t} \in T$. The IP model then follows as

$$\min \quad \sum_{(ij) \in A} \widetilde{c}_{ij} y_{ij} - \sum_{t \in T} k_\mu \mu_t z_t, \tag{8}$$

$$\text{such that} \quad y_{ij} = \sum_{h=0}^{C_N} x_{ij}^h \quad \forall\, (i, j) \in A, \tag{9}$$

$$\sum_{i \in N_t^-} x_{it}^{h-1} = \sum_{j \in N_t^+} x_{tj}^h \quad \forall\, t \in T, h = 1, \ldots, C_N, \tag{10}$$

$$\sum_{t \in T} z_t \leq C_T, \tag{11}$$

$$\sum_{i \in N_t^-} y_{it} \geq z_t \quad \forall\, t \in T, \tag{12}$$

$$\sum_{j \in N_i^-} y_{ji} = \sum_{j \in N_i^+} y_{ij} \leq 1 \quad \forall\, i \in N, \tag{13}$$

$$\sum_{d \in D} \sum_{j \in N_d^+} y_{dj} = 1, \tag{14}$$

$$y_{ij} + y_{kl} \leq 1 \quad \forall\, ((i, j), (k, l)) \in \Gamma, \tag{15}$$

$$z_{\bar{t}} = 1, \tag{16}$$

$$x_{ij}^h \in \{0, 1\} \quad \forall\, (i, j) \in A, h = 0, \ldots, C_N, \tag{17}$$

$$y_{ij} \in \{0, 1\} \quad \forall\, (i, j) \in A, \tag{18}$$

$$z_t \in \{0, 1\} \quad \forall\, t \in T. \tag{19}$$

In (9), the dependent variable y is defined in terms of x, enabling more concise and readable formulation of constraints (12)–(15). Consider three consecutive nodes i, t, j in $N(q)$. By constraint (9), $x_{tj}^{\bar{h}} = 1$ for a unique hop index $\bar{h} = 0, \ldots, C_N$, and constraint (10) enforces the hop-index for which $x_{tj}^{h} = 1$ to be $\bar{h} + 1$. Observe that (10) does not apply to the substation nodes D. As a result, $|N(q)| \leq C_N$, and path q has no cycles disconnected from the substation nodes.

The inequality (11) imposes the upper bound C_T on $|T(q)|$, and constraint (12) assures that $t \in T(q)$ only if $t \in N(q)$. Constraints (13) ensure that each turbine node has a predecessor in q if and only if it has a successor node in the path, and that the predecessor and successor nodes are unique if they exist. Existence and uniqueness of a substation in $N(q)$ is guaranteed by constraint (14), and arc crossings are avoided by (15). The generated path q is finally enforced to connect turbine $\bar{t}$ by constraint (16).

3.4. A path-generating algorithm

In the following, a solution algorithm is developed. In each of its iterations, the algorithm solves instances of the continuous relaxation of the master problem (1)–(4), and exploits the optimal values of the dual variables to define new instances of the subproblem. Paths found as optimal solutions to the latter problem instances induce new variables and constraints to be supplied to the master problem instance. As each addition of a new path leads to generation of both a new column and a new non-crossing constraint, traditional column- or row-generation techniques do not apply.

A set $\bar{T}$ of target turbines that are to be connected by some new path (see constraint (16)) is considered in the algorithm. In the outer loop, $\bar{T}$ is assessed, *e.g.* by random selection, and each $\bar{t} \in \bar{T}$ is processed in an inner loop. By solution of (8)–(19), a path q connecting $\bar{t}$, and possibly other turbine nodes, is generated. If q is not already included in $\bar{P}$, the path set is extended by q.

Parameters k_μ and k_η are applied in order to diversify the path generation. Multiplication by their respective terms in the objective function (8) adjusts the contribution from the dual values μ and η. The algorithm is enabled to modify both parameters in each iteration of the inner loop. The iterative procedure is stated in Algorithm 1.

Recall from Section 2 that a path p is understood as a set of turbines $T(p)$ that some cable connects, in addition to a sequence $N(p)$ of nodes from a substation, via nodes visited by the cable (including $T(p)$), and back to the substation. For each $d \in D$ and $t \in T$ such that $(d, t) \in A$, the first step of Algorithm 1 finds the path p consisting of node sequence (d, t, d) and connected turbine set $T(p) = \{t\}$, and includes it in the set $\bar{P}$ of paths. Assume that this initial step yields a path set $\bar{P}$ for which the master problem has a feasible solution. This assumption is reasonable as long as, for all $t \in T$, $(d, t) \in A$ for the substation node minimizing c_{dt}.

In each iteration of the outer loop (lines 4–18), searches for new paths are made. The inner loop (lines 6–14) iterates over the target turbines, and searches for a new connecting path for each. This is accomplished by solving a corresponding subproblem instance (line 8), which depends on the current estimate of optimal values of μ and η. If the search is successful, information about arcs crossing the new path is recorded (lines 10–13), and the path set $\bar{P}$ is extended (line 14). Finally, in all outer iterations but the last, the relaxation of the master problem is solved again in order to obtain updated optimal values of the dual variables μ and η.

Ideally, the stopping criterion of the outer loop should be $z(\bar{P}) \geq 0$ (see 6), *i.e.* the non-existence of a path $q \in P \setminus \bar{P}$ for which the objective function takes a negative value. To allow for interruption before optimality is proved, the algorithm is stated in terms of a general stopping criterion. Relevant examples include stopping once a sufficient number of paths has been generated, and stopping when the number of outer iterations has reached an upper bound. Once the criterion is satisfied, the non-relaxed version of the master problem is solved, which yields an optimal subset $\bar{P}^*$ of the generated paths $\bar{P}$. The effect of the number of outer iterations on the result is examined in Section 4.

Algorithm 1

1: Let $\bar{P}$ be the set of paths $p \in P$, where $N(p) = (d, t, d)$, $T(p) = \{t\}$, $d \in D$ and $t \in T$
2: **for** all $p \in \bar{P}$, let $\bar{\chi}_p$ be the set of paths in $\bar{P}$ crossing path p
3: Initiate μ and η to zero
4: **repeat**
5:     Let $\bar{T}$ be a set of target turbines in T
6:     **for** all target turbines $\bar{t} \in \bar{T}$ **do**
7:         Assign values to parameters k_μ and k_η
8:         Solve subproblem (8)–(19) to obtain a path q, with $\bar{t} \in T(q)$
9:         **if** $q \notin \bar{P}$ **then**
10:            Calculate the modified embedding $\widetilde{L}(q)$ as defined in Section 3.3.3
11:            Calculate the set $\xi_q \subseteq A \setminus A(q)$ of arcs crossing the perturbed embedding $\widetilde{L}(q)$
12:            Let $\bar{\chi}_q = \{p \in \bar{P} : A(p) \cap \xi_q \neq \emptyset\}$ be the set of paths in $\bar{P}$ crossing path q
13:            **for** all $p \in \bar{\chi}_q$, add path q to $\bar{\chi}_p$
14:            Add path q to $\bar{P}$
15:     **if** the stopping criterion is not satisfied **then**
16:         Solve the continuous relaxation of master problem (1)–(4) to assess μ and η
17:         Update the objective function coefficients in (8) with the new values of μ and η
18: **until** the stopping criterion is satisfied
19: Solve the master problem (1)–(4) with integrality constraints

---

4. Numerical experiments

4.1. Implementation

The master problem, the subproblem, and Algorithm 1 are implemented in Python® 3.6, using the GUROBI™ 8 Python bindings for defining and solving the (integer) linear programs. The algorithm is implemented such that the paths are generated in parallel in the inner loop (see Section 3.4). This is accomplished with the Python `multiprocessor` library, starting parallel instances of the GUROBI solver in separate processes. Random choices for parameters are implemented such that they are evaluated in a deterministic order, and, with the random generator initialized by a seed, such that they are reproducible. Each instance of the subproblem, as well as the master problem, are solved to optimality. An upper bound on the number of outer iterations is applied as the stopping criterion in Algorithm 1.

4.2. Experiments

Turbine and substation layouts of the *Barrow 1* and *Sheringham Shoal* wind farms (Klein and Haugland 2019) are the targets of the numerical experiments. The *Barrow 1* wind farm has one substation and 30 turbines, while *Sheringham Shoal* has two substations and 88 turbines. All numerical experiments are conducted on a virtual machine with 32 CPUs and 118 GB memory.

Four parameters of the algorithm have to be assigned values. Besides the factors k_μ and k_η defining the weight of the dual values, and the set $\bar{T}$ of target turbines, the bound on the number of outer iterations must be assessed. Let the bounds C_N and C_T on the path size vary within a certain range in each experiment, such that $C_T + 2 \leq C_N \leq C_T + 4$.

4.2.1. A small wind farm with one substation

In the first set of experiments, the layout data of the *Barrow 1* wind farm are considered. The cable capacity is set to $C_T = 4$, and the bound on the total number of turbines visited by a cable is set to $C_N = 6$. In each outer iteration of Algorithm 1, the set of target turbines is $\bar{T} = T$. Parameters k_μ and k_η are assigned identical values, and k is adopted as a notation of their joint value. In the first experiment, the cable length produced by the algorithm is investigated in terms of a function of k and the bound on the number of iterations.

Results hence obtained are compared with the solutions found in the second set of experiments: the values of k_μ and k_η are drawn randomly from a uniform distribution on the interval $[0, 1]$. Both values are drawn independently for each instance of the subproblem to be solved.

The solutions obtained are listed in Table 2. For each value of k, 30 iterations of the algorithm were processed in less than 20 minutes. It is seen from the numbers in brackets that, for all examined values of k, almost all paths generated in early iterations of the algorithm are distinct. The maximum possible number of unique paths after five iterations is 180 (30 initial one-turbine paths, and 30 paths per iteration), and for most values of k around 160, distinct paths were generated. However, for fixed values of the parameter k, after iteration 10 almost all generated paths are duplicates of earlier paths, *i.e.* no new paths are generated. There is thus little benefit in using more than 15 iterations for a fixed value of k in this particular instance. As expected, in the experiment with $k = 0$, *i.e.* where μ and η do not contribute to the subproblem, the subproblem instances in each outer iteration are identical, and no new paths are generated.

Independent random values of k_μ and k_η in each subproblem yield the best experimental results. This holds true both in terms of a larger number of generated paths and in terms of smaller total cable lengths. This observation does not come as a surprise, as one of the main challenges in a path-based algorithm is the generation of paths of sufficient diversity. The cable layout computed for this choice of parameter values, in the case of $C_T = 5$ and $C_N = 7$, is depicted in Figure 4. It is seen that eight cables are used, two of which connect a single turbine.

It is further investigated how the computation time of the algorithm varies with the cable capacity C_T and the maximum number C_N of visited turbines. Random values of k_μ and k_η are generated as explained above. The set of target turbines $\bar{T}$ is generated by drawing 16 turbine nodes from T, all with equal probability, and with repetitions disallowed. A random set is hence found at the start of each outer iteration of Algorithm 1.

The results from this experiment are documented in Table 3. A strong correlation between the solution time and the bound C_N on the number of visited turbines is observed. In addition, the required computation time increases with increasing differences between C_N and the bound C_T on the number of connected turbines per cable. The significant increase in running time with increasing values of C_N is expected, as the number of variables in the subproblem increases linearly with C_N.

4.2.2. A larger wind farm with two substations

The *Sheringham Shoal* instance is subject to the last set of experiments. Figure 5 visualizes one of the computed cable layouts of this wind farm.

Table 2. Results for *Barrow 1*, $C_T = 4$, $C_N = 6$. The table shows the optimal total cable length in metres, and the number of generated unique paths in brackets, for different numbers of outer iterations and values of k.

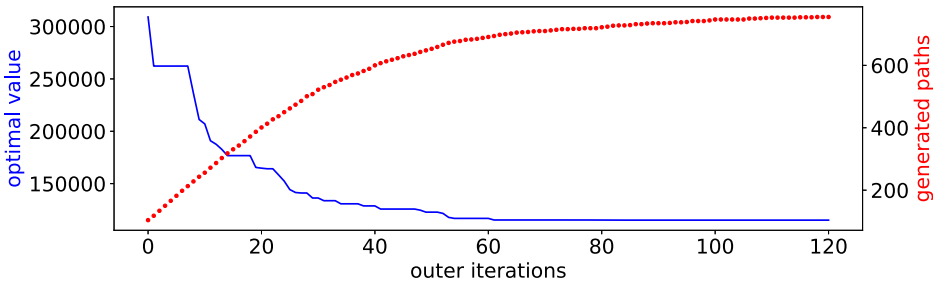|	Total cable length and number of generated paths						
Iteration	$k = 0$	$k = 0.2$	$k = 0.4$	$k = 0.6$	$k = 0.8$	$k = 1.0$	random k_η, k_μ
1	86238 [59]	86238 [59]	86238 [59]	86238 [59]	86238 [59]	86238 [59]	86238 [59]
2	86238 [59]	70816 [77]	62191 [86]	76004 [86]	76004 [86]	76004 [86]	68188 [83]
5	86238 [59]	57147 [139]	56774 [161]	54470 [161]	56146 [163]	53186 [163]	52819 [158]
10	86238 [59]	50185 [155]	49315 [202]	47142 [231]	46814 [231]	48974 [233]	47393 [237]
20	86238 [59]	50185 [155]	49315 [202]	47142 [234]	46814 [234]	48974 [235]	44606 [273]
30	86238 [59]	50185 [155]	49315 [202]	47142 [234]	46814 [234]	48974 [235]	44606 [275]
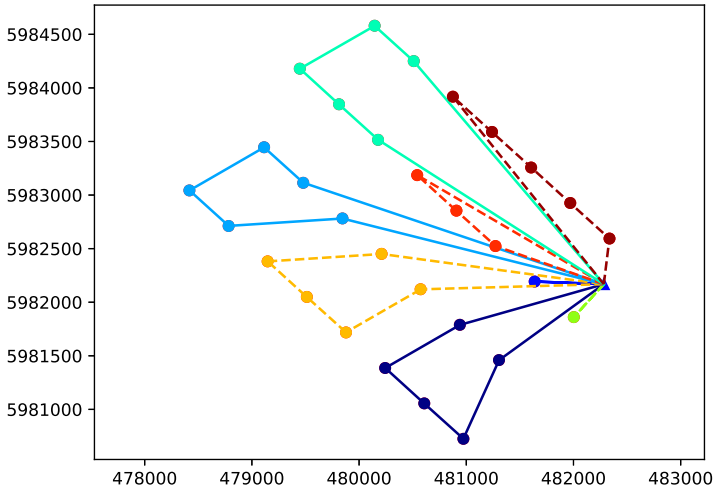
Figure 4. Solution with eight cable lines at the *Barrow 1* wind farm, computed with $C_T = 5, C_N = 7$, 30 iterations, paths for 16 random turbines per iteration, and independent random values for k_η and k_μ. The turbines are illustrated as circles, and the connecting cables are depicted as solid and dashed lines. The triangle represents the substation.

Table 3. Results for *Barrow 1*, with k_μ and k_η random, and the subproblem solved for 16 randomly chosen target turbines in each iteration. The table shows the required time (in minutes:seconds) to perform 10 iterations of Algorithm 1.

	Running time				
C_T	$C_N = 4$	$C_N = 5$	$C_N = 6$	$C_N = 7$	$C_N = 8$
4	0:14	0:48	2:29	7:58	26:47
5	–	0:34	1:22	4:03	12:41
6	–	–	0:57	2:30	4:30
7	–	–	–	2:09	3:29
8	–	–	–	–	2:38
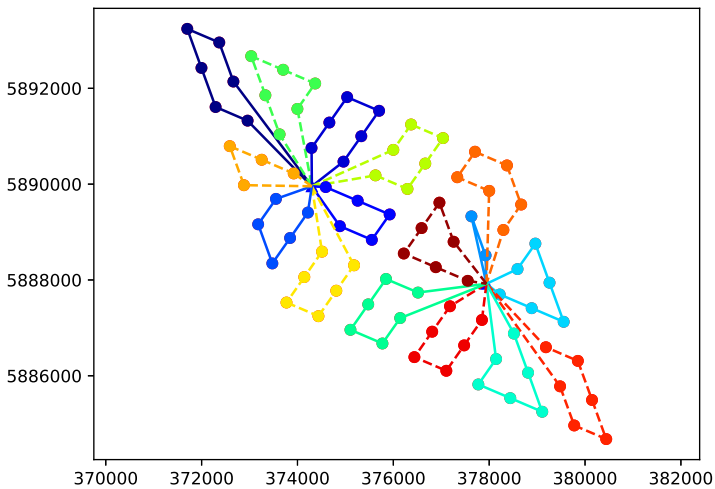
Figure 5. Solution with 16 cables at the *Sheringham Shoal* wind farm, computed with $C_T = 6, C_N = 7$, 80 iterations, paths for 16 random turbines per iteration, and independent random values for k_η and k_μ. The turbines are illustrated as circles, and the connecting cables are depicted as solid and dashed lines. The triangles represent the substations.

Figure 6. Total cable length (solid line) and number of generated unique paths (dotted line) as a function of the number of outer iterations, for a cable layout of the wind farm *Sheringham Shoal*.

A significant increase in the computational burden for this larger instance is observed, where the number of nodes is $|N| = 88$. This is partially due to the larger number of paths that must be generated, but also due to higher computational costs for solving the subproblem instances. A cable layout corresponding to the bounds $C_T = 5$ and $C_N = 7$ is also computed. The parameters k_μ, k_η and $\bar{T}$ are assigned random values, as explained in the previous experiment. In addition, the execution time of the IP-solver is limited to 300 seconds in each subproblem instance. If a feasible solution is found, the corresponding path q is processed according to steps 9–14 of Algorithm 1. Otherwise, the inner iteration turns out to be unproductive. With these settings, processing 120 outer iterations took 7 hours.

In Figure 6, the total cable length and the number of generated unique paths are depicted as a function of the number of outer iterations. It is observed that the algorithm performs well in generating new unique paths that have not been previously generated in the first 40–60 iterations. At higher outer iteration counts, the number of calculated new unique paths decreases, as a significant amount of the generated paths are duplicates of already existing ones.

5. Conclusions

The current work introduces a novel solution approach for computing offshore wind farm cable layouts. Building on a model based on decision variables associated with feasible cable paths, the approach combines a module for the selection of paths with a module for the generation of new paths. Corresponding optimization models, referred to as the master problem and the subproblem, respectively, are also introduced. Optimal values of the dual variable in the continuous relaxation of the master problem are incorporated as cost or revenue coefficients in the objective function of the subproblem. It is shown that, by perturbing the weights assigned to these coefficients, the diversity in the paths generated is improved.

Experiments demonstrate that a small number of distinct paths can be sufficient for the computation of complete reliable cable layouts. In the instances tested, the methodology presented mainly generates paths that are good solution candidates, as the number of paths is a small fraction of the number of possible paths in the network.

The resulting layouts, illustrated in Figures 4 and 5, demonstrate the capability of the algorithm presented here. An important feature of the methodology proposed is its handling of non-crossing constraints, where it optimizes the extent to which cables are partly laid in parallel following a joint trajectory. It seems reasonable to assume that this feature becomes more prominent in wind farms of a size beyond that considered in the current experiments. In larger instances, more turbines may have to be connected to the same substation. This creates a congestion of cables in close proximity to the substation, and thereby an increased risk of cable routes that appear as obstacles to other cables. Such cases are likely to benefit more extensively from opportunities to let multiple cables partly follow the same route.

The computational cost of solving the subproblem is high for wind farms with a large number of turbines. Instances with large cable capacity, measured in terms of the number of turbines to which the cables can connect, are particularly hard to solve. The running time of the solution process is largely dominated by the generation of new paths in the subproblem. Further development of the algorithm should therefore be focused on this part. One strategy in this direction would thus be to develop an heuristic method for solving the subproblem, while pursuing the other components of the solution approach.

It is highly relevant to integrate decisions concerning turbine locations and cable layout in one model. The path-based modelling approach studied in this article is likely to be suitable for such integration. Optimization methods intended for optimal placement of turbines often perturb the positions of some turbines only slightly from one iteration to the next. Algorithms with this characteristic motivate the reuse of cable paths, computed in earlier iterations of the turbine layout problem. The most time-consuming part of the methodology presented, the generation of new paths, can thus be entirely or partially omitted. Mathematical models and computational methods for integration of the current approach with optimization of turbine locations are left as topics for future research.

Disclosure statement

Funding

References

Bauer, Joanna, and Jens Lysgaard. 2015. "The Offshore Wind Farm Array Cable Layout Problem: A Planar Open Vehicle Routing Problem." *Journal of the Operational Research Society* 66 (3): 360–368.

Cerveira, Adelaide, José Baptista, and E. J. Solteiro Pires. 2016. "Wind Farm Distribution Network Optimization." *Integrated Computer-Aided Engineering* 23 (1): 69–79.

Cerveira, Adelaide, Amaro de Sousa, E. J. Solteiro Pires, and José Baptista. 2016. "Optimal Cable Design of Wind Farms: The Infrastructure and Losses Cost Minimization Case." *IEEE Transactions on Power Systems* 31 (6): 4319–4329.

Chen, Ying, Hua Li, Kai Jin, and Qing Song. 2013. "Wind Farm Layout Optimization Using Genetic Algorithm with Different Hub Height Wind Turbines." *Energy Conversion and Management* 70: 56–65.

Chowdhury, Souma, Jie Zhang, Achille Messac, and Luciano Castillo. 2013. "Optimizing the Arrangement and the Selection of Turbines for Wind Farms Subject to Varying Wind Conditions." *Renewable Energy* 52: 273–282.

CleanTechnica. 2019. *Vattenfall Wins 760 Megawatt Subsidy-Free Dutch Offshore Wind Tender*. Technical report. https://cleantechnica.com/2019/07/11/vattenfall-wins-760-megawatt-subsidy-free-dutch-offshore-wind-tender.

Dong Energy. 2017. *DONG Energy Awarded Three German Offshore Wind Projects.* https://orsted.com/en/Company-Announcement-List/2017/04/1557851.

Du Pont, Bryony L., and Jonathan Cagan. 2012. "An Extended Pattern Search Approach to Wind Farm Layout Optimization." *Journal of Mechanical Design* 134 (8): Article ID 081002. doi:10.1115/1.4006997.

Emami, Alireza, and Pirooz Noghreh. 2010. "New Approach on Optimization in Placement of Wind Turbines within Wind Farm by Genetic Algorithms." *Renewable Energy* 35 (7): 1559–1564.

Fagerfjäll, Patrik. 2010. "Optimizing Wind Farm Layout—More Bang for the Buck Using Mixed Integer Linear Programming." Master's thesis, Chalmers University of Technology and Gothenburg University.

Fischetti, Martina, and David Pisinger. 2018a. "On the Impact of Considering Power Losses in Offshore Wind Farm Cable Routing." In *Operations Research and Enterprise Systems*, edited by Greg H. Parlier, Federico Liberatore, and Marc Demange, 267–292. Cham, Switzerland: Springer International.

Fischetti, Martina, and David Pisinger. 2018b. "Optimal Wind Farm Cable Routing: Modeling Branches and Offshore Transformer Modules." *Networks* 72 (1): 32–59.

Fischetti, Martina, and David Pisinger. 2018c. "Optimizing Wind Farm Cable Routing Considering Power Losses." *European Journal of Operational Research* 270 (3): 917–930.

Fischetti, Martina, and David Pisinger. 2019. "Mathematical Optimization and Algorithms for Offshore Wind Farm Design: An Overview." *Business & Information Systems Engineering* 61 (4): 469–485. doi:10.1007/s12599-018-0538-0.

Gong, Xuan, Stefanie Kuenzel, and Bikash C. Pal. 2018. "Optimal Wind Farm Cabling." *IEEE Transactions on Sustainable Energy* 9 (3): 1126–1136.

González, J. S., A. G. Gonzalez Rodriguez, J. C. Mora, J. R. Santos, and M. B. Payan. 2010. "Optimization of Wind Farm Turbines Layout Using an Evolutive Algorithm." *Renewable Energy* 35 (8): 1671–1681.

Gonzalez-Longatt, Francisco M., Peter Wall, Pawel Regulski, and Vladimir Terzija. 2012. "Optimal Electric Network Design for a Large Offshore Wind Farm Based on a Modified Genetic Algorithm Approach." *IEEE Systems Journal* 6 (1): 164–172.

Grady, S. A., M. Y. Hussaini, and M. M. Abdullah. 2005. "Placement of Wind Turbines Using Genetic Algorithms." *Renewable Energy* 30 (2): 259–270.

Herbert-Acero, José F., Oliver Probst, Pierre-Elouan Réthoré, Gunner Chr. Larsen, and Krystel K. Castillo-Villar. 2014. "A Review of Methodological Approaches for the Design and Optimization of Wind Farms." *Energies* 7 (11): 6930–7016.

Hertz, Alain, Odile Marcotte, Asma Mdimagh, Michel Carreau, and François Welt. 2017. "Design of a Wind Farm Collection Network when several Cable Types are Available." *The Journal of the Operational Research Society* 68 (1): 62–73.

Ituarte-Villarreal, Carlos M., and Jose F. Espiritu. 2011. "Optimization of Wind Turbine Placement Using a Viral Based Optimization Algorithm." *Procedia Computer Science* 6: 469–474.

Klein, A., and D. Haugland. 2019. "Obstacle-Aware Optimization of Offshore Wind Farm Cable Layouts." *Annals of Operations Research* 272 (1-2—Special Issue: Advances in Theoretical and Practical Combinatorial Optimization): 373–388. doi:10.1007/s10479-017-2581-5.

Klein, A., D. Haugland, J. Bauer, and M. Mommer. 2015. "An Integer Programming Model for Branching Cable Layouts in Offshore Wind Farms." In *Modelling, Computation and Optimization in Information Systems and Management Sciences*, Vol. 359 of *Advances in Intelligent Systems and Computing*, edited by H. A. Le Thi, T. Pham Dinh, and N. T. Nguyen, 27–36. Cham, Switzerland: Springer International. doi:10.1007/978-3-319-18161-5_3.

Larsen, G. C., H. A. Madsen, N. Troldborg, T. J. Larsen, P.-E. Réthoré, P. Fuglsang, S. Ott, *et al.* 2011. *TOP-FARM—Next Generation Design Tool for Optimisation of Wind Farm Topology and Operation*. Technical report Risø-R-1805(EN), National Laboratory for Sustainable Energy, Denmark Technical University, Risø, Denmark. https://backend.orbit.dtu.dk/ws/portalfiles/portal/10328531/ris_r_1805.pdf.

Lindahl, M., N. C. F. Bagger, T. Stidsen, S. F. Ahrenfeldt, and I. Arana. 2013. "OptiArray from DONG Energy: An Automated Decision Support Tool for the Design of the Collection Grid in Large Offshore Wind Power Plants." In *Proceedings of the 12th Wind Integration Workshop—International Workshop on Large-Scale Integration of Wind Power into Power Systems as well as on Transmission Networks for Offshore Wind Power Plants*. Langen, Germany: Energynautics. http://windintegrationworkshop.org/wp-content/uploads/sites/11/2016/02/WIW13_Proceedings_Content_Overview.pdf.

Lingling, H., F. Yang, and G. Xiaoming. 2009. "Optimization of Electrical Connection Scheme for Large Offshore Wind Farm with Genetic Algorithm." In *2009 International Conference on Sustainable Power Generation and Supply*. Piscataway, NJ: IEEE. doi:10.1109/SUPERGEN.2009.5348118.

Marmidis, Grigorios, Stavros Lazarou, and Eleftheria Pyrgioti. 2008. "Optimal Placement of Wind Turbines in a Wind Park Using Monte Carlo Simulation." *Renewable Energy* 33 (7): 1455–1460.

Mosetti, G., C. Poloni, and B. Diviacco. 1994. "Optimization of Wind Turbine Positioning in Large Windfarms by Means of a Genetic Algorithm." *Journal of Wind Engineering and Industrial Aerodynamics* 51 (1): 105–116.

Pillai, A. C., J. Chick, L. Johanning, and M. Khorasanchi. 2018. "Offshore Wind Farm Layout Optimization Using Particle Swarm Optimization." *Journal of Ocean Engineering and Marine Energy* 4 (1): 73–88.

Pillai, A. C., J. Chick, L. Johanning, M. Khorasanchi, and V. de Laleu. 2015. "Offshore Wind Farm Electrical Cable Layout Optimization." *Engineering Optimization* 47 (12): 1689–1708.

Pillai, A. C., J. Chick, L. Johanning, M. Khorasanchi, and S. Pelissier. 2016. "Optimisation of Offshore Wind Farms Using a Genetic Algorithm." *International Journal of Offshore and Polar Engineering* 26 (3): 225–234.

Pillai, A. C., J. Chick, M. Khorasanchi, S. Barbouchi, and L. Johanning. 2017. "Application of an Offshore Wind Farm Layout Optimization Methodology at Middelgrunden Wind Farm." *Ocean Engineering* 139: 287–297.

Quan, Ning, and Harrison M. Kim. 2019. "Greedy Robust Wind Farm Layout Optimization with Feasibility Guarantee." *Engineering Optimization* 51 (7): 1152–1167.

Quinonez-Varela, G., G. W. Ault, O. Anaya-Lara, and J. R. McDonald. 2007. "Electrical Collector System Options for Large Offshore Wind Farms." *IET Renewable Power Generation* 1 (2): 107–114. https://www.researchgate.net/publication/3481406_Electrical_collector_system_options_for_large_offshore_wind_farms.

Rodrigues, S., P. Bauer, and Peter A. N. Bosman. 2016. "Multi-Objective Optimization of Wind Farm Layouts—Complexity, Constraint Handling and Scalability." *Renewable and Sustainable Energy Reviews* 65: 587–609.

Shin, Je-Shok, and Jin-O. Kim. 2017. "Optimal Design for Offshore Wind Farm Considering Inner Grid Layout and Offshore Substation Location." *IEEE Transactions on Power Systems* 32 (3): 2041–2048. doi:10.1109/TPWRS.2016.2593501.

Svendsen, H. 2013. "Planning Tool for Clustering and Optimised Grid Connection of Offshore Wind Farms." *Energy Procedia* 35: 297–306.

The Kingfisher Information Service—Offshore Renewable & Cable Awareness Project (KIS-ORCA). 2016a. *London Array Offshore Wind Farm*. Technical report. http://www.kis-orca.eu/media/67068/LondonArray_LRes.pdf.

The Kingfisher Information Service—Offshore Renewable & Cable Awareness Project (KIS-ORCA). 2016b. *Robin Rigg Offshore Wind Farm*. Technical report. http://www.kis-orca.eu/media/9340/RobinRigg_LRes.pdf.

Wędzik, Andrzej, Tomasz Siewierski, and Michał Szypowski. 2016. "A New Method for Simultaneous Optimizing of Wind Farm's Network Layout and Cable Cross-Sections by MILP Optimization." *Applied Energy* 182: 525–538.

Wei, Shurong, Lu Zhang, Yao Xu, Yang Fu, and Fangxing Li. 2017. "Hierarchical Optimization for the Double-Sided Ring Structure of the Collector System Planning of Large Offshore Wind Farms." *IEEE Transactions on Sustainable Energy* 8 (3): 1029–1039.

WindEurope. 2017. *Wind in Power 2017*. Technical report. http://windeurope.org/wp-content/uploads/files/about-wind/statistics/WindEurope-Annual-Statistics-2017.pdf.

Zhang, Peter Y., David A. Romero, J. Christopher Beck, and Cristina H. Amon. 2014. "Solving Wind Farm Layout Optimization with Mixed Integer Programs and Constraint Programs." *EURO Journal on Computational Optimization* 2 (3): 195–219. doi:10.1007/s13675-014-0024-5.